Erosion of solid neon by keV electrons

J. Schou, P. Børgesen,* O. Ellegaard, and H. Sørensen
Department of Physics, Association EURATOM—Risø National Laboratory, P.O. Box 49, DK-4000 Roskilde, Denmark

C. Claussen
Fysisk Institut, Odense Universitet, DK-5230 Odense M, Denmark
(Received 23 December 1985)

The erosion of solid neon by keV electrons has been studied experimentally and theoretically. Electronic sputtering as well as temperature-enhanced sublimation are investigated by a frequency-change measurement on a quartz crystal or in some cases by the change in intensity of reflected electrons. The erosion yield increases with increasing temperature for substrate temperatures above 7 K. Below this temperature sputtering via electronic transitions is the dominant process. The yield shows a clear minimum for film thicknesses about $(5-7)\times10^{16}$ Ne atoms/cm^2 for 2-keV electrons. The sputtering yield for thick films has a maximum at 1.2—1.5 keV. The results are explained by the diffusion of excitations to the surface with subsequent decay. From this model and the experimental results one derives a characteristic diffusion length of about 1×10^{17} Ne atoms/cm^2. The eventual particle ejection is driven by decay of surface-trapped excitons or by dissociative recombination. The magnitude of the yield indicates that deexciting neon particles at the surface induce further sputtering. Direct sputtering from electron-nucleus collisions does not contribute significantly to the yield.

I. INTRODUCTION

The erosion of condensed gases by ions or electrons plays an important role in many fields. In interstellar and planetary atmospheric problems the recent laboratory data for erosion are expected to have implications for the competition of collection and loss of volatiles by icy bodies in space.[1-3] In technological problems such as cryopumping in radiation environments,[4] the phenomenon has also turned out to be important. A particular case is the study of erosion of hydrogen pellets in a plasma.[5,6]

The erosion of condensed gases by charged particles has been investigated intensively during the past years.[2,7-12] The types of phenomena studied range from electronic sputtering alone to beam-induced evaporation at high current densities or at high temperatures. Most of the experiments have been performed for ion bombardment, and the results typically exceed the estimates of ordinary sputtering theory[13] by orders of magnitude. There is little doubt that the large erosion yields for the condensed gases are essentially caused by the energy initially deposited in electronic excitations. However, in addition, there may be a significant contribution from nuclear stopping for sufficiently low energy ions. Various models, more or less related to electron-stimulated desorption, have been presented in an attempt to explain how the energy is transferred to atomic motion.[9,10,14-18] Sputtering via electronic transitions is well known from irradiation of alkali halides,[19] for which the yield is above ten at electron bombardment below 1 keV at temperatures of about 600 K.

Measurements of the erosion of solid rare gases as a result of particle bombardment have been carried out by several groups.[2,7,9,15,16,20,21] Energy spectra of ejected particles from ion-bombarded solid argon[22] and krypton[11,22] have been reported as well. In addition, some erosion measurements have been combined with or performed by luminescence studies.[12,15,16,23] These studies complement a large number of studies on luminescence from electron-irradiated solid rare gases, e.g., Refs. 24—27.

Several of these experiments demonstrate clearly that there is a close connection between electronic sputtering and luminescence for solid neon and argon. Brown *et al.* measured the electronic sputtering of solid argon as a result of MeV light-ion bombardment, and correlated the thickness dependence of the yield with the emission of the strong 9.8-eV line from exciton decay in argon.[15,16] They indicated that the processes leading to particle ejection were primarily a generation of hole-electron pairs, diffusion of holes, and subsequent dissociative recombination close to the surface. An additional contribution to the yield was ascribed to the radiative decay of molecular argon excitons to the repulsive ground state. This latter mechanism for converting electronic excitations into atomic motion was suggested previously by the present authors,[18,20] and a significant effect was predicted for argon-doped solid neon.

The erosion yield at electron bombardment turned out to be a factor of 2 larger for pure solid neon than for neon with even very small amounts of impurities. This effect was explained by the reduced diffusion length of the free excitons in solid neon.[20] A similar decrease in the sputtering yield for argon was observed after doping with oxygen.[16] Coletti *et al.*[12] measured the correlation between luminescence intensity and the condensation rate of argon on graphite during low-energy-electron bombardment. They demonstrated that the sputtering rate was proportional to the density of vibrationally excited, molecular ex-

citons at the surface.

In many respects, neon deviates from the heavier rare gases. The band gap is considerably larger[28,29] ($\approx$21.6 eV) and the bottom of the conduction band lies higher above the vacuum level in neon ($V_0 \approx 1.3$ eV) than in solid argon[28] ($V_0 \approx 0.4$ eV). Contrary to all the heavier rare gases, a large fraction of the excitons in neon are present as atomic excitons.[24,27,30,31] The magnitude of this fraction has turned out to be strongly influenced by the type of primary excitation, e.g., x-ray irradiation or bombardment by low-energy electrons.[30,32] For solid neon, vibrational relaxation of molecular excitons Ne_2^* shows up to be very inefficient compared to molecular excitons in, for example, solid argon, but the relative population of the vibrational levels also depends on the sample quality and on the location of the trapped exciton in the sample.[30] Furthermore, the diffusion lengths for optically excited free molecular excitons in solid neon have turned out to be more than 1 order of magnitude larger than for argon.[33]

In the present work we have studied the erosion of solid neon for a variety of experimental parameters. In several respects neon is one of the most appropriate materials for electron-induced erosion (and sputtering) of all: The yield is high, and the thickness dependence of the yield is weak above 2×10^{17} Ne atoms/cm^2. On the other hand, solid neon is so volatile that all experiments have to be performed close to liquid-helium temperature. Poor heat conduction from the substrate to the cooling aggregate will immediately lead to beam-induced evaporation from the solid neon.[7]

The erosion has been studied by two independent methods described previously:[7] The fortuitous combination of a large yield and an atomic mass, which is not too small, means that erosion of neon by keV electrons could be studied systematically with a quartz-crystal microbalance (the frequency-change method). In addition, a large number of measurements were performed by determining the number of electrons needed to remove the neon film from a massive gold substrate. The variation of the electron emission was used here to indicate when the film had been eroded away (the emissivity-change method). Neon is also well suited to this method, since the yield of high-energy secondaries (the reflection coefficient) varies by a factor of 2 from thick films of neon to the gold substrate.

The present work contains a short description of the experimental setup and of the two methods used. The first systematic experimental results for neon are presented and discussed in view of the existing theoretical models. In particular, we shall discuss possible deexcitation modes that may provide energy for the particle ejection.

II. EXPERIMENTAL SETUP AND METHODS

The basic experimental setup as well as the methods utilized have been described in great detail recently.[7,17] Here we shall only briefly outline the principles.

A film of solidified neon is produced by letting a jet of cooled gas impinge on a massive gold target plate or on an oscillating quartz crystal (Fig. 1). In both cases the substrate is cooled to a temperature close to that of liquid helium. For deposition on the crystal the film thickness is determined directly from the frequency change, whereas the thickness for the massive target plate is determined by a careful calibration procedure. A typical deposition rate was 3×10^{15} Ne atoms/cm^{2}sec. A film may be removed rapidly just by heating the target area with an electric heater.

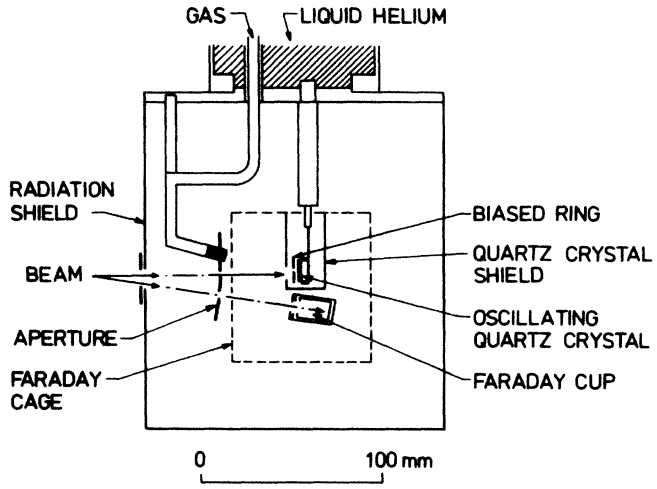

FIG. 1. Schematic drawing of the target region of the experimental setup. The quartz crystal may be replaced by a massive target plate.

Beams of (1–3)-keV electrons are obtained from a small electron gun, and swept horizontally and vertically by two independent sawtooth voltages over a 2-mm aperture in front of the target, thus ensuring a homogeneous irradiation of a large part of the target area. It is known that the erosion profile in the film resembles a truncated frustum of a right circular cone.[7] The substrate is partially heated by the incident electron beam, but care is taken to keep the temperature about or below 6 K, where the erosion is insensitive to target temperature. The current density was usually kept below 10 μA/cm^2, where the evaporation caused by beam heating is insignificant.[7]

The target plate as well as the crystal are electrically insulated from the cryostat, and during irradiation the target current will generally differ from the true beam current because of the emission of secondary and reflected electrons (and possibly ions). A negative bias of -45 or -90 V applied to a very open grid or merely a repeller ring will suppress almost all secondary-electron emission. The true beam current is measured by deflecting the beam into a Faraday cup below the target area. The target region and the Faraday cup are both located inside an electrically grounded Faraday cage. Cup, cage, grid (or repeller ring), and quartz-crystal shield are all heated to temperatures sufficiently high to prevent the gas from condensing on them. In this manner we attempt to minimize disturbing effects from areas that may charge up.

The *frequency-change method* utilizes the possibility of measuring instantaneously the mass change on a quartz-crystal microbalance during particle bombardment. The increasing frequency is measured during erosion, and the slope of the frequency curve may then be applied to a direct determination of the erosion yield for a known

beam current. An example is shown in Fig. 2 for two different grid voltages. For both curves one notes an almost linear part which corresponds to a yield of approximately 30 Ne atoms per electron. A typical film deposition of 4×10^{17} Ne atoms/cm^2 on the silver electrode corresponds to a frequency shift of approximately 600 Hz. The subsequent erosion by the beam results in a frequency increase of about 150 Hz, which means that only a fraction of the total deposited mass is removed. In this way we obtain a satisfactory determination of the spatial extension of the erosion spot as well.

The *emissivity-change* method exploits the variation of the secondary-electron emission from the target for decreasing film thicknesses. In particular, the total number of electrons that are necessary to obtain the electron emission characteristic for the substrate (i.e., to remove the film) may be determined. We define an "electron-emission coefficient" η by

$$i_t^- = (1-\eta) i_b \ , \tag{1}$$

where i_b is the beam current measured with the cup and i_t^- the target current for a negative bias. The reflected electrons characterized by η will still have sufficient energy to escape. For thicknesses less than half the electron range, η increases almost linearly with decreasing thickness from the value of bulk neon ($\sim$0.2) to that of the gold or silver substrate ($\sim$0.4). The reflection coefficients depend slightly on the primary energy, but the method is applicable for the energies considered here.

The erosion yield Y for an initial thickness x is evaluated from

$$Y(x) \approx N \frac{d(Ax)}{d\Phi} \ , \tag{2}$$

where N is the number density, A the eroded area, and Φ the total number of electrons necessary for a complete erosion.[7] The area A must be found from another method, e.g., from the frequency-change method.

The measurements with the frequency-change method enable us to determine the erosion yield in a straightforward manner, but the thermal conduction between the cryostat and the beam-impact area on the crystal has to be sufficiently good, so that unnecessary heating of the area is avoided. This may be controlled by comparing the results to those from the emissivity-change method applied to an ordinary, massive plate with good thermal conduction to the cryostat (and thermometer). The disadvantages of the emissivity-change method are that the erosion must continue until the substrate is reached, and that one requires knowledge of the area of the eroded spot. However, the two methods supplement each other, and in many cases have been used simultaneously for erosion measurements.

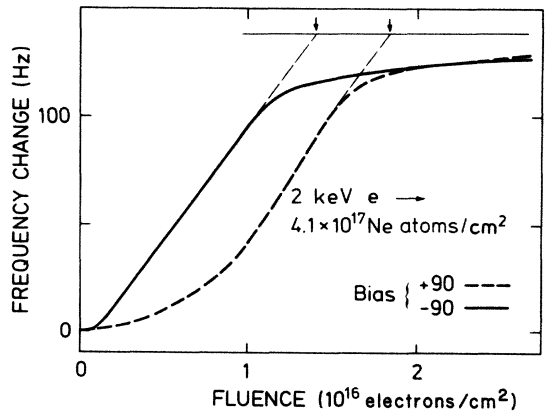

FIG. 2. Erosion of a 4.1×10^{17}-(Ne atoms/cm^2) thick film on a quartz crystal by 2-keV electrons. The frequency change is plotted versus fluence. Grid bias, + 90 V (— — —) and −90 V (——). The arrows indicate the fluence necessary for a complete erosion.

A direct comparison between the two methods is possible if the linear part of the frequency curve is prolonged as shown in Fig. 2: The intercept between the linear part and the asymptotic level determines a fluence necessary for completing the erosion. Since one evaluates the fluence for the erosion measurements with the emissivity-change method in a similar way, one may compare the fluences obtained from the two methods.[7]

Since the erosion of solid neon has appeared earlier to be sensitive to the presence of small impurities, the gas inlet tube was cooled down to temperatures for which only neon and hydrogen can pass. Contamination with hydrogen and deuterium was minimized, e.g., by heating the cryogenic system to room temperature before experiments with neon.

III. EXPERIMENTAL RESULTS

In the following subsections we shall describe the dependence of the yield on several experimental parameters, as well as the agreement between the results obtained by the two different methods.

A. Dependence on grid voltage

Practically all erosion measurements on the present setup have been performed with a negatively biased grid (−45 or −90 V). Apart from neon and argon all materials investigated so far show no dependence on the grid voltage. Since many of the solidified gases are insulating materials with high secondary-electron emission coefficients, charge-up problems during erosion may be substantially reduced by such a negative bias.

In Fig. 2 the erosion of a Ne film with positive and negative grid bias is shown. One notes that the yield during the linear part of the erosion is essentially identical for both voltages, but since the erosion with positive bias increases much more slowly than the one with negative bias, the necessary fluence for an erosion becomes more than 30% larger with positive bias.

This result has been confirmed through a number of measurements with the emissivity-change method for other film thicknesses and electron energies. The fluence with positive bias is usually larger, occasionally by more than a factor of 3.

The fluence is influenced by the magnitude of the positive grid bias as well. Measurements with the emissivity-change method have demonstrated that the fluence does

not vary for grid voltages from -100 up to about $+10$ V. Then the fluence increases drastically in the interval from 10 to 30 V. For voltages larger than 30 V no further enhancement of the fluence takes place.

We have chosen mainly to consider the erosion yield obtained with negative bias. Since the maximum yields during an erosion are similar, one then avoids the complex behavior with a "delay" in the erosion for positive bias. Results obtained with the frequency-change method are then compared with those with the emissivity-change method. One notes that the curve in Fig. 2 measured with negative bias is almost linear during most of the erosion.

B. Comparison between the two methods

Results obtained by the two methods—frequency and emissivity change—are shown in Fig. 3. The initial thickness has been depicted as a function of the fluence necessary to complete the erosion. Only points obtained for an erosion on a quartz crystal are directly indicated. Fluences measured for a gold as well as a silver electrode are shown, and in some cases simultaneous results obtained with the emissivity-change method are included. The average erosion yield from previous emissivity-change measurements on a massive gold target is indicated as well. One notes the convincing agreement for all thicknesses.

The agreement between the results obtained by the two methods on a massive gold target and on a quartz crystal demonstrates that the surface of the quartz crystal apparently is so cold that essentially no beam-induced evaporation takes place.

According to Eq. (1), one may estimate the yield for 2-keV electrons on neon from the slope of the curve produced by the data points. The slope shown in Fig. 3 corresponds to a yield of ~ 28 Ne atoms/electron.

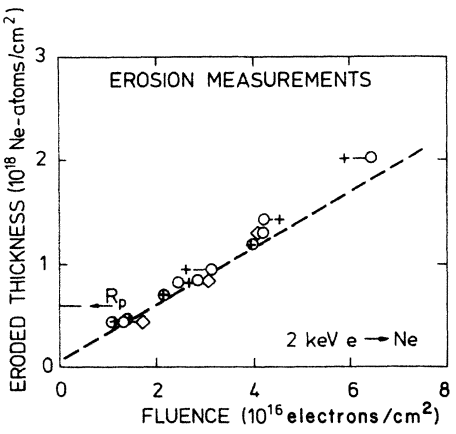

FIG. 3. Sputtering measurements by the emissivity-change and the frequency-change method for 2-keV electrons incident on neon. The eroded thickness is plotted versus the fluence necessary for an erosion (cf. Fig. 2). +, frequency change for a Ag electrode as substrate; ◇, frequency change for a Au substrate; ○, simultaneous emissivity-change measurements; — — —, previous results on a massive Au substrate by the emissivity-change method. (The beam-spot area for the two latter ones is taken from the frequency-change method.) R_p is the estimated range of 2-keV electrons in neon.

C. Dependence on temperature

As described in the previous subsection, one has to ensure that the erosion is performed below the temperature regime in which the erosion yield increases with temperature. This is conveniently done by the emissivity-change method using a massive gold substrate that is heated by an electrical heater. Because of the good heat conduction from the heater (and the thermometer) to the interface, we are able to determine the substrate temperature. The precise temperature at the beam spot on the film is, of course, known only approximately. The thermometer was approximately calibrated, so temperatures are uncertain (on an absolute scale) by ± 0.2 K.

In Fig. 4 the yield has been depicted as a function of the average substrate temperature. The results have been obtained by the emissivity-change method for a film thickness of 3.2×10^{17} Ne atoms/cm^2, corresponding to a value not too far from the thickness-independent region (cf. Sec. III D). The yield is seen to increase with substrate temperature above about 6 K.

The sublimation flux from an isothermal surface as estimated from Eq. (5) (Sec. IV B) is included in Fig. 4. For the primary current used, one may estimate the sputtered flux to about 5×10^{13} Ne atoms/sec. The sublimation flux from the irradiated area (≈ 7 mm^2) then exceeds the sputtered flux at temperatures above 8 K. One notes the similar increase for the sublimation flux and the flux of eroded particles.

D. Dependence on film thickness

Results for 2-keV electrons incident on neon films deposited on the quartz crystal are shown in Fig. 5. These points have all been determined by the frequency-change method, since the variation of η with film thickness below 1×10^{17} Ne atoms/cm^2 is insufficient.

One notes the clear minimum slightly below 1×10^{17} Ne

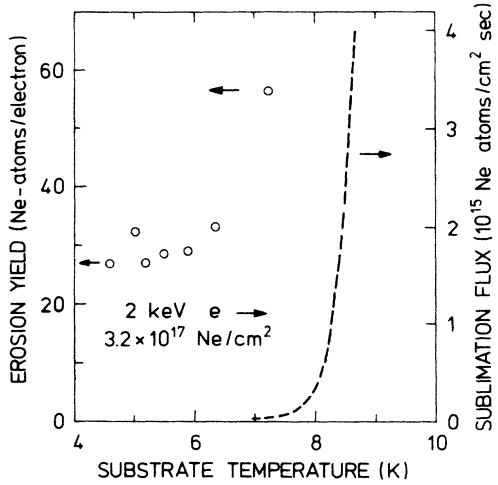

FIG. 4. Erosion of a 3.2×10^{17}-(Ne atoms/cm^2)-thick film on a massive gold plate by 2-keV electrons. The yield [Eq. (2)] is plotted versus the substrate temperature. The beam-spot area has been normalized as in Fig. 3. — — —, sublimation flux [Eq. (5)].

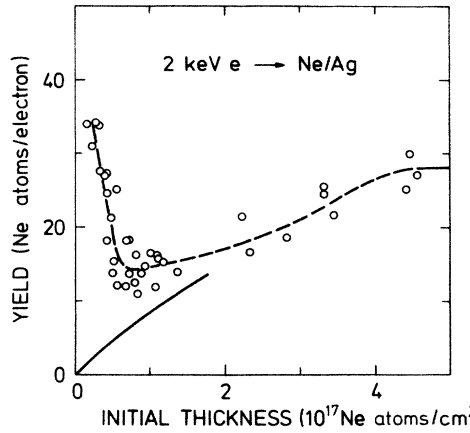

FIG. 5. Sputtering yield of solid neon resulting from bombardment of 2-keV electrons measured by the frequency-change method. The yield is plotted versus the initial thickness. The silver electrode of the crystal serves as a substrate. — — —, curve drawn to guide the eye. ——, Eq. (20) with $ff_e=3$ and $l_0=1\times10^{17}$ Ne atoms/cm^2.

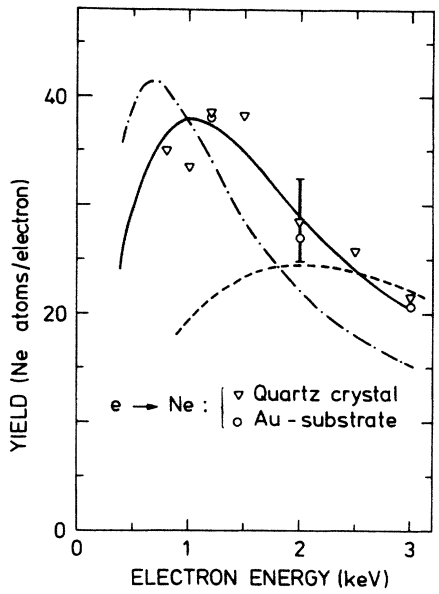

FIG. 6. Sputtering of 4.5×10^{17}-(Ne atoms/cm^2)-thick films by keV electrons. The yield is plotted versus the primary electron energy. Only the average value is indicated at each energy. ▽, the frequency-change method with the standard deviation indicated at 2 keV. o, the emissivity-change method with the beam-spot area as in Fig. 3. — — —, calculated yield from Eq. (16), $l_0=3\times10^{17}$ Ne atoms/cm^2 and $ff_e=1$; ——, $l_0=1\times10^{17}$ Ne atoms/cm^2 and $ff_e=3$; —·—, $l_0=0.5\times10^{17}$ Ne atoms/cm^2 and $ff_e=5$.

atoms/cm^2, and the slowly increasing yield from this minimum up to approximately 4.5×10^{17} Ne atoms/cm^2. Above this thickness almost no further enhancement takes place. The strong increase for decreasing thicknesses below the minimum leads to a thin-film yield that exceeds the "bulk" yield of ~28 Ne atoms/electron substantially. For practical reasons the measurements were carried out on several crystal holders of slightly different construction, but the data show the same trend. A similar behavior with a minimum positioned at about the same thickness was observed for 3-keV electrons.

For these measurements we have utilized only the initial yield, as the cone profile of the eroded film makes it difficult to deduce a proper thickness dependence during the later stages of an erosion. For example, the high yield for small film thicknesses may easily be hidden in statistical fluctuations in the frequency during the erosion of thick films.

E. Energy dependence

The yield of a 4.5×10^{17}-(Ne atoms/cm^2) film is shown in Fig. 6 as a function of primary energy. The data have been obtained either by the frequency-change method on a quartz crystal with a silver electrode or by the emissivity-change method with a massive gold substrate.[20] The thickness investigated is close to the thickness-independent regime, and comparable to the range of 1.7-keV electrons in materials of similar atomic number, e.g., nitrogen and oxygen.[34,35]

The yield curve has a maximum approximately at 1.2—1.5 keV, and decreases with increasing energy almost proportionally to the stopping power. The general trend is similar for the two different kinds of data points. The previous data[20] were underestimated by a constant factor of about 2.5 that accounts for the actual magnitude of the eroded area.[7] These measurements were carried out only down to the primary energy 1.2 keV because of insufficient beam intensity. Unfortunately, it was not possible to carry out reliable measurements at energies below 0.8 keV because of beam-adjustment problems.

F. Influence of impurities

Recent measurements with the emissivity-change method on an ordinary gold substrate demonstrated that a small amount of impurities may increase the fluence necessary for an erosion by more than a factor of 2.[20]

Examples of such sputtering measurements are shown in Fig. 7. The reference measurement with pure neon was performed before any argon was let in. The other two measurements were carried out with films contaminated with argon. The contaminant was either regularly added to the neon gas in the gas container or merely present in the cryostat from previous runs with doped neon films. The sputtering is apparently much slower for the contaminated neon film.

A sequence of sputtering measurements on argon-doped neon films were performed in this way for concentrations that varied from 0.05 to 5 at.% argon (in the gas container before inlet to the cryostat). The results indicated no clear dependence on the argon content, except for large concentrations. Apparently, the fluence decreased with the concentration above an argon content of 1 at.%.[20]

In these measurements the gas tube in the cryostat has to be heated to a temperature that allows the less volatile argon to enter into the target region as well. In the reference measurements with pure neon the tube was also heated in order to keep the experimental parameters practical-

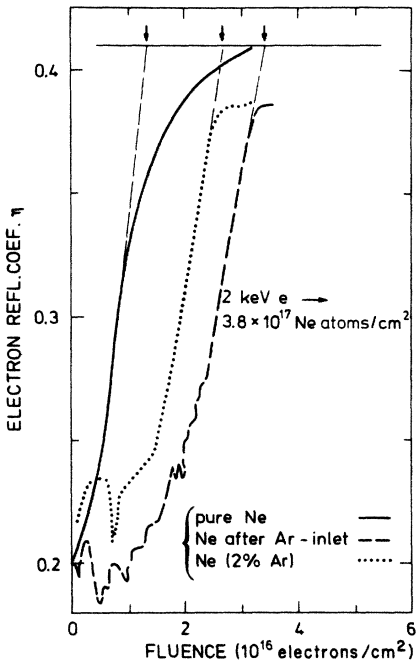

FIG. 7. Sputtering of 3.8×10^{17}-(Ne atoms/cm^2)-thick films by 2-keV electrons. The electron-reflection coefficient is plotted versus the fluence. The measurements have been performed by the emissivity-change method on a massive Au substrate. ——, for a pure neon film; — —, for a neon film deposited after a previous argon inlet; · · ·, for a neon film doped with 2 at. % argon.

ly identical. These measurements were difficult to reproduce with the frequency-change method. The film deposition on a massive gold substrate at elevated gas-tube temperature is probably largely different from that on a silver electrode of a quartz crystal because of the different surface conditions.

G. Comparison with other measurements on condensed gases

The slow sputtering of solid neon with a positive *bias* compared to a negative one has no parallel in erosion of other condensed gases.[7]

A strong dependence of the yield on the *temperature* has been observed for the solid rare gases argon and xenon.[9,21] Although the enhancement of the yield occurs at much higher temperatures for these much less volatile gases, the general trend is similar for all these targets.

The effect of an increasing *current density* on the erosion yield has also been considered by several groups.[9,21]

A dependence on the film *thickness* has been observed for solid rare gases at MeV-ion bombardment.[9,15,16,21] In all cases the yield reaches the "bulk" value between 2×10^{17} and 4×10^{17} atoms/cm^2. In particular, for xenon on a beryllium substrate the yield is found to increase, as is also seen for neon above 1×10^{17} atoms/cm^2 (Fig. 5). The sputtering of xenon on a 2000-Å layer of frozen SF_6, on the other hand, resulted in a clearly decreasing yield with increasing film thickness. For nitrogen and oxygen bombarded by electrons, the yield only decreases slightly with thickness.[17]

The *energy dependence* of the yield for light MeV ions on solid argon was previously asserted to be proportional to the square of the stopping power,[9] but recent measurements on argon show a linear dependence rather than a quadratic dependence on the stopping power.[16] With the present setup, not only the yield of solid neon for energies above 1.5 keV, but also the yield of nitrogen and oxygen, seems to be almost proportional to the stopping power for the primary electrons.[17]

The *magnitude* of *the yield* for neon at 2 keV is significantly larger than the corresponding electron-induced yield of 8 D_2-molecules/electron for solid deuterium[7] in spite of the much larger sublimation energy for the former (20 meV/Ne-atom) compared to 12 meV/D_2-molecule. The yield is even comparable to that for solid hydrogen.[36]

IV. THEORY I: DIRECT SPUTTERING AND BEAM-INDUCED EVAPORATION

The solid rare gases are all characterized by the weak interatomic van der Waals binding, corresponding to sublimation energies from 0.17 eV/atom for xenon down to 0.02 eV/atom for neon.[28] This low-energy value means that any electronic excitation or initiated atomic motion in neon may lead to a *high* sputtering yield, even if the mechanism involved has a low efficiency. In addition, the maximum energy transfer to a neon atom in an electron-nucleus collision for a keV electron is an order of magnitude larger than the surface binding energy. Furthermore, beam-induced sublimation may, of course, also easily contribute to the erosion yield because of this low binding energy.

In the present section we shall consider two possible mechanisms for erosion: (A) sputtering resulting from electron-nucleus collisions, and (B) erosion caused by beam heating or external heating. Sputtering via electronic transitions will be treated in Sec. V.

A. Direct electron sputtering

It is well known that sputtering resulting from direct electron-nucleus collisions may occur.[37] Since most metals have a surface binding energy of a few eV, beam energies in the MeV regime are usually necessary for a significant sputtering yield. This process is, of course, analogous to ordinary ion-induced sputtering, in which the kinetic energy is transferred directly from the primary atom to target atoms.

A 2-keV electron may transfer up to 0.2 eV to a neon nucleus at rest. With an efficiency of 1 (which, of course, is strongly overestimated) this would lead to a yield of 10 Ne atoms per such an event. The actual total yield from direct sputtering obviously depends strongly on the scattering cross section. In order to estimate the cross section we shall adopt the nonrelativistic expression from Berger *et al.*[38] for the differential cross section for elastic scattering:

$$\frac{d\sigma}{d\Omega}=\frac{Z^2e^4}{4E^2(1-\cos\theta+2\eta_s)^2}K_{\rm rel}(\theta)\ , \tag{3}$$

where θ is the deflection angle and K_{rel} a factor (≈ 1) that includes spin and relativistic effects. As usual, Z is the atomic number and e the elementary charge. The screening parameter η_s has been evaluated to

$$\eta_s = 1.7\times 10^{-5} Z^{2/3}/[\tau(\tau+2)] , \quad (4)$$

where τ is the kinetic energy in units of the electron rest energy. A scattering in which a 2-keV electron transfers energy greater than $U_0 = 20$ meV to a neon nucleus corresponds to a scattering process in which the deflection angle exceeds $\theta \approx 10°$. Even though the angle is comparatively small, the cross section for this is about 2×10^{-17} cm^2. This means that such a collision happens on the average solely 8 times within the thickness 4×10^{17} Ne atoms/cm^2, from which the processes obviously contribute the yield, following Fig. 5. Since small scattering angles are dominant, and since any sequence of recoiling nuclei initiated by the struck nucleus is unable to transfer energy over thicknesses comparable to the electron range, at most a minor fraction of the yield may originate from this direct process. Although we have ignored the slowing down of primaries (and the subsequent enhancement of the scattering cross section), we may definitely consider sputtering via electronic transitions to be far more important.

B. Erosion by heating

Evaporation as a result of beam heating or external heating has been reported in several experiments.[7,9,21,39–41] Such a mechanism has even occasionally been asserted to be the dominant process.[21,42] In any case, it is clear that evaporation may contribute to the total yield, and even exceed the nonthermal component from beam-induced electronic transitions by more than several orders of magnitude.

The yield increase caused by substrate heating was estimated from the sublimation flux from an isothermal surface in Sec. III C. This estimate was used for solid argon to explain the temperature dependence of the yield as well.[9] The evaporation flux Ψ is given by

$$\Psi(T) = \gamma P(T)(2\pi M k_B T)^{-1/2} , \quad (5)$$

where γ is the condensation efficiency ($\gamma \approx 1$), $P(T)$ the sublimation pressure at the temperature T, k_B Boltzmann's constant, and M the mass of an neon atom.

We note that any reliable erosion on solid neon without substantial sublimation has to be performed on a substrate below 7 K.

The yield increase Y_{sp} (where sp denotes spike) as a result of high current density is well described by the late-stage component of a low-temperature spike:[43]

$$Y_{sp} = \frac{1}{J}[\Psi(T_a + \Delta T_{eff}) - \Psi(T_a)] , \quad (6)$$

where J is the current density, T_a the ambient target temperature, and ΔT_{eff} the average temperature rise of the target. The evaporation rate $\Psi(T)$ (number of evaporated atoms per unit time and area) may be estimated from experimental data on vapor pressure from the solidified gases, e.g., by use of Eq. (5).

The starting point for the spike treatment is a variation of a well-known problem in the mathematical theory of heat transfer. An initial heat pulse along a track perpendicular to the surface results in a temperature increment of cylindrical geometry in the semi-infinite medium. The temperature rise at the surface leads then to an enhanced evaporation.

The solution to the problem reduces to Eq. (6) if the initial heat input is sufficiently low, e.g., a stopping power of the order of 1 eV per 10^{15} atoms/cm^2. In addition, the temperature rise ΔT_{eff} due to the beam has to be considerably lower than the ambient temperature T_a.

The best agreement to the yield increase Y_{sp} was obtained for $T_a = 6.6$ K and $\Delta T_{eff} = 0.13J$ K (J in μA/cm^2). This corresponds to a temperature rise of about 1 K up to 4.5 K at the highest current density. Then, the temperature in the beam spot for low current densities is estimated to be about 7 K, which agrees well with the data from the massive gold substrate. In the cylindrical spike model this invokes a characteristical duration of the evaporation of the order of

$$t_{max} = \frac{\Delta T_{eff} C}{J(dE/dx)} , \quad (7)$$

where C is the heat capacity per unit volume and dE/dx the stopping power. t_{max} is about 100 μsec. The alternative case of a hemispherical spike, however, leads to a time of the order of 1 sec.

Later, the theoretical treatment[43] was extended to include heat loss through the boundary by evaporation,[44] but this does not change the previous results for low-temperature cylindrical spikes. The crater form is predicted to be very flat, i.e., the depth should be small compared to the lateral extension. A large lateral expansion of the beam spot up to an area 3–4 times larger than the usual beam spot has indeed been observed at the highest current densities.[7]

It should be noted that the erosion that takes place in our case at elevated current densities is fundamentally different from the laser-induced sputtering of oxides and compound semiconductors, where a similar energy-density dependence of the sputtering yield was observed.[45] This enhancement is definitely ascribed to the effect of dense electronic excitations.

V. THEORY II: SPUTTERING BY ELECTRONIC TRANSITIONS

The major problem in the sputtering of insulating materials is how the energy expended in electronic excitations and ionizations becomes available for atoms as kinetic energy.

A. Sputtering from electronic excitations: Constant density

Let us now regard sputtering from noble gases in terms of diffusion of excitations and subsequent *decay*[14,15,18,20] (Fig. 8). Electronic excitation and ionization by fast-charged particles in solid rare gases are known to produce luminescence from exciton decay.[26,28] However, a consid-

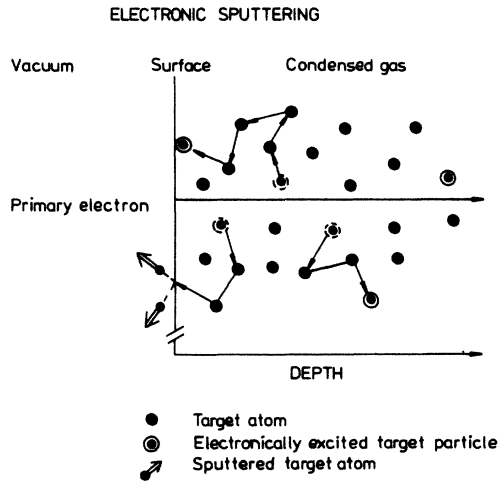

FIG. 8. Schematic drawing of electronic sputtering from electron incidence. The density of excited target particles is greatly exaggerated.

erable part of the total energy of excitons is not released as radiation, but transferred to the lattice through electronic deexcitations to repulsive states and multiphonon processes. The excitons in solid rare gases are highly mobile prior to self-trapping,[28] and a similar mobility has recently been asserted for the holes.[15]

In Ref. 20 we regarded the vibrationally excited molecular exciton R_2^* as the main "carrier" of electronic energy. In the following treatment we shall derive results for sputtering originating from diffusion of excitations in a more general manner.

Let us consider an unspecified electronic excitation, e.g., a molecular exciton or a hole-electron pair, generated by charged-particle irradiation. We assume that this excitation may diffuse in a way similar to that of the lowest-lying excitons.[46] The concentration $C(\mathbf{r},t)$ of the free excitations must satisfy the diffusion equation

$$D\nabla^2 C=\frac{\partial}{\partial t}C+\frac{1}{\tau}C\ . \tag{8}$$

We further assume the initial condition

$$C(\mathbf{r},0)=n_0\delta(y)\delta(z)\ \text{ for } x>0\ , \tag{9}$$

i.e., constant depth density n_0 of excitations along the track at the time $t=0$. The latter term on the right-hand side of Eq. (8) represents the drain from the population, e.g., for mobile excitons or holes because of trapping or deexcitation. The diffusion constant D and the characteristic lifetime τ of the excitations in the mobile state are as usual related to the diffusion length $l_0=(D\tau)^{1/2}$. The δ functions $\delta(y)$ and $\delta(z)$ fix the impact of the primary in (0,0,0). The initial condition (9) corresponds to a uniform excitation density along the track of a charged particle as expected for a projectile with constant stopping power, e.g., a MeV proton up to quite large depths.

Equation (8) is solved by standard methods[18] for a semi-infinite medium, for which the plane $x=0$ corresponds to the surface. As a boundary condition, the surface is considered to be absorbing, i.e., C vanishes here:

$$C(0,y,z,t)=0\ \text{ for } t>0\ . \tag{10}$$

This boundary condition has been used in previous analyses of exciton diffusion.[46] The flux

$$j=-\left[-D\frac{\partial C}{\partial x}\right]_{x=0} \tag{11}$$

of excitations arriving at the surface then leads immediately to a total number of excitations,

$$\int_0^\infty dt\int dy\int dz\, j=n_0 l_0\ , \tag{12}$$

all of which originate from the single-particle track described by Eq. (9).

The diffusion equation utilized here is completely equivalent to the treatment given by Ophir *et al.*[46] and Reimann *et al.*,[15] although these authors predominantly considered steady-state excitation. Reimann *et al.* applied a reflecting surface as a boundary condition similar to that suggested by Schwentner *et al.*[47] from photoelectron-emission experiments. In our case the use of a reflecting surface leads to a yield that is much too small (cf. Sec. VI C).

In the case of a film of finite thickness, the system of equations has to be extended by an additional boundary condition for the film-substrate interface at $x=d$. As in all related work,[15,46,47] we regard the interface between the film and the metal substrate as absorbing in a manner analogous to Eq. (10). This leads to a modification of Eq. (12) by a factor $\tanh(d/2l_0)$.[18]

The number of excitations per depth, n_0, may be estimated by

$$n_0=fNS_e/W\ , \tag{13}$$

where N is the number density, S_e the electronic stopping cross section, and W the average energy expended to make a hole-electron pair. f is the number of this specific excitation per hole-electron pair, i.e., $f=1$ for diffusion of holes. (Note that the meaning of f is more general than that of Ref. 20.)

The total yield from an infinitely thick film then becomes

$$Y=(fNS_e/W)l_0 p f_e\ , \tag{14}$$

where p is the emission probability for an atom through a surface with a planar barrier about equal to the sublimation energy.[18] f_e indicates the average number of *ejected* atoms per deexcited molecule or atom at the surface, e.g., by a low-energy cascade as in the treatment suggested by Reimann *et al.*[15] Since the energy release at the surface from deexcitation is generally much larger than the sublimation energy, p is very close to unity for neon and argon.[18] Therefore, in the following treatment we usually neglect the factor p. We note that the bulk yield is proportional to the stopping power NS_e and to the diffusion length l_0. This result was presented in Ref. 20 as well.

The possible processes that lead to particle ejection at the surface will be considered in Sec. V C.

B. Diffusion of excitations for electron incidence

The simple approach, for which the excitation density has the constant value fNS_e/W along the track, is not applicable for electron bombardment. It is well known that the distribution of energy deposited in excitation and ionization varies considerably as a function of depth.[38,48] Furthermore, it is clear that the finite range of the electrons has to be included in the calculation. These two restrictions were not included in Ref. 20.

We approximate the distribution of electronic excitations by a Gaussian density for an electron of primary energy E:

$$n^*(\mathbf{r})=(fE/W)G(x)\delta(y)\delta(z)\ , \tag{15a}$$

where

$$G(x)=(2\pi\sigma_D^2)^{-1/2}\exp[-(x-r_D)^2/(2\sigma_D^2)]\ . \tag{15b}$$

fE/W is the number of excitations produced by the primary, and $r_D(E)$ and $\sigma_D(E)$ the mean range and standard deviation of the distribution. The latter two quantities are determined primarily by the atomic number of the target. As a good approximation both quantities may be regarded as proportional to the range. The reason for this is that the distribution of electronically deposited energy is very insensitive to variations of the primary energy, once the distribution is depicted in units of the stopping power $NS_e(E)$ versus the range $R_e(E)$ (cf. Ref. 48). Then the yield for an infinitely thick film becomes

$$Y=\tfrac{1}{2}(f_e fE/W)\exp(\sigma_D^2/2l_0^2-r_D/l_0)\times\operatorname{erfc}[\sigma_D/(\sqrt{2}l_0)-r_D/(\sqrt{2}\sigma_D)]\ , \tag{16}$$

where erfc is the complementary error function. This expression is depicted in Fig. 6 for several values of l_0 and the product ff_e.

We note that the ratios σ_D/l_0 and r_D/l_0 enter as arguments for the exponential function. For a fixed l_0 it means as expected that a broad distribution or a small mean range will lead to a large yield. The mean range r_D and the standard deviation σ_D for neon may be estimated from data for materials of similar atomic numbers.

From close inspection of the distribution of deposited energy for 2-keV electrons in atmospheric air in Ref. 38, we may then determine the proportionality constants

$$r_D=0.375R_e(E) \tag{17a}$$

and

$$\sigma_D=0.34R_e(E)\ . \tag{17b}$$

$R_e(E)$ is the extrapolated practical range in Ref. 38, which is in good agreement with the experimentally determined range in solid nitrogen[34] or oxygen.[35]

This relatively simple approach for large film thicknesses is unsuitable for small thicknesses, for which two modifications become necessary. The first important point is the additional boundary condition for an interface in the plane $x=d$, similar to the case of constant excitation density. If the atomic numbers of the condensed-gas film and the substrate are similar, the distribution of deposited energy becomes only slightly distorted relative to the distribution in a bulk film. Then, the Gaussian distribution (15) is still appropriate, and the yield becomes[49]

$$Y=(ff_eE/W)\left[\int_0^d G(x)\exp(-x/l_0)dx-\exp(-d/l_0)[\sinh(d/l_0)]^{-1}\times\int_0^d G(x)\sinh(x/l_0)dx\right]\ . \tag{18}$$

For the case of thin films on a widely different substrate, e.g., neon on a silver electrode, one has to use a completely different estimate for the excitation density in the film. We ignore the slowing down of primaries in the film, and let $r(E_0)\cos\theta_0 dE_0 d\cos\theta_0$ be the number of electrons reflected from the substrate with energy E_0 and polar angle θ_0 per primary. In this approximation we have utilized the knowledge that the reflected electrons exhibit a cosine distribution.[50] The total energy deposited by the primary and the backscattered electrons in the film then becomes

$$d\left[NS_e(E)+\int_0^E r(E_0)NS_e(E_0)dE_0\right]\ . \tag{19}$$

The first term in the large parentheses is the energy loss of the primary, and in the integral every reflected electron contributes with the energy $dNS_e(E_0)/\cos\theta_0$. Then, we obtain, for the total yield,

$$Y=(ff_e/W)\left[NS_e(E)+\int_0^E r(E_0)NS_e(E_0)dE_0\right]\times l_0\tanh(d/2l_0)\ . \tag{20}$$

For small thicknesses the yield increases with increasing film thickness d, and one notes that the yield for very thin films ($d/l_0\ll 1$) is independent of the diffusion length l_0. The approximation behind Eq. (20) is at least valid up to thicknesses of more than 1×10^{17} Ne atoms/cm^2 at the primary energy 2 keV. For larger thicknesses the excitation density increases considerably as a result of the slowing down and scattering of the primaries. The sum in the large parentheses has been evaluated on the basis of a known electron spectrum, $r(E_0)$,[51] and a semiempirical compilation of the stopping power $NS_e(E_0)$ for neon.[52] The result for 2 keV is $1.5NS_e(E)$, which means that the backscattered electrons on the average deposit half as much energy as the incident ones at the surface.

C. Energy-release processes

The fundamental channels of deexcitation of hole-electron pairs and excitons in solid neon[30,53–55] may end up in lattice distortions or sputtering. These processes occur even for transitions with an energy release of about or below 100 meV, since the sublimation energy for neon (and for argon) is comparatively low. Below we shall consider some of the possible processes which provide energy for atomic motion. The mobility of the excitations is discussed in Sec. VI.

The energy loss from keV electrons to electronic excitations is caused mainly by ionization processes of atoms and molecules,[56,57] i.e., for condensed gases by the

creation of hole-electron pairs. A hole will be localized as the molecular state Ne_2^+:[53,55]

$$Ne^+ + Ne \rightarrow Ne_2^+ . \quad (21)$$

By capturing an electron the molecular hole $A\,^2\Sigma_u^+$ forms a highly excited molecule Ne_2^{**}, which instantaneously decays nonradiatively to the free $3p$ exciton[55] or to the $3p$ self-trapped atomic exciton[53] (Fig. 9):

$$Ne_2^+ + e^- \rightarrow Ne_2^{**} \rightarrow Ne + Ne^*(3p) . \quad (22)$$

The decay sequence indicated by Inoue *et al.*[55] is shown in Fig. 9 as I, whereas the sequence suggested by Belov *et al.* is shown as II. About 1.1 eV is liberated by the decay of Ne_2^{**} after electron capture to the vibrationally relaxed state of Ne_2^+. Of course, more energy is released if the electron capture takes place for a vibrationally excited Ne_2^+, i.e., up to the dissociative energy for Ne_2^+ 1.3 eV extra.[58]

The luminescence spectrum from particle- or photon-irradiated solid neon is characterized by the lines from self-trapped atomic or molecular excitons, whereas the decay of free $3s$ excitons so far has not been observed.[28] The atomic self-trapped excitons occur both in the bulk and at the surface.[27] Fugol' *et al.*[26,59] estimate that the shift induced by the transition from $4s$ to the ground state $3p^6\,^1S$ in argon is about 0.2 eV, which is available for sputtering. An estimate for solid neon based on their tables leads to a shift of about 0.05 eV resulting from the radiative transition $3s$ to $2p^6\,^1S$ (IV in Fig. 9).

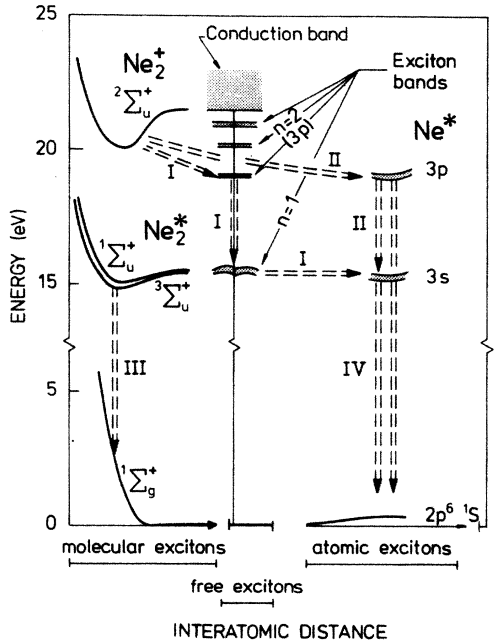

FIG. 9. Schematic representation of the important potential-energy curves. The arrows on the X axis indicate increasing interatomic distance. The bands in the middle between the molecular excitations and the atomic excitons show the position of the *free*-exciton bands and the conduction band in solid neon. The transitions indicated by dashed arrows are explained in the text. The design of the figure is taken from Ref. 53.

Let us now estimate the energy release from molecular self-trapped excitons. In solid neon these excitons occur predominantly in highly vibrationally excited states.[30,60] The relaxation to low-lying states by multiphonon processes is inefficient because of the large energy difference between the vibrational states compared with the phonon energies.[28,30] Furthermore, the transition rate is reduced substantially for molecular excitons at the surface or in small crystallites in the bulk of layers deposited by evaporation.[30] The radiative transition from the vibrationally relaxed $^{1,3}\Sigma_u^+$ molecular states to the ground state imparts about 3.7 eV of kinetic energy on the average to the two atoms[18] (see process III in Fig. 9). The decay from the *excited* levels transfers up to 0.5 eV extra energy to the atoms.[28]

The ratio of the number of atomic to molecular self-trapped excitons depends heavily on the type of the primary excitation.[30] Surface-sensitive excitation leads to an enhancement of the number of the atomic excitons relative to the molecular ones. In our previous work on solid neon[20] we utilized the ratio of intensities $(I(Ne_2^*)/[I(Ne^*)+I(Ne_2^*)]\approx 0.35)$ determined by Packard *et al.*[24] Their sample was irradiated by electrons from a tritiated external source. From the recent work by Coletti *et al.*,[27] we find a similar ratio for bombardment by 2.5-keV electrons. We note that the decay channel via these molecular self-trapped excitons is efficient for sputtering because of the comparatively large energy release.

Recently, Coletti *et al.*[12] suggested that the ejection was a result of a relaxation of a cavity with a self-trapped exciton. The minimizing of the elastic strain of the crystal and of the surface energy of the cavity at the sample surface will liberate sufficient energy for atomic motion, e.g., about 1 eV for Ar_2^*.[12]

VI. DISCUSSION: ELECTRONIC SPUTTERING

The thickness dependence of the yield in Fig. 5 indicates that two mechanisms may operate during electronic sputtering. The large yield at small thicknesses would then have another origin than the yield for thicknesses larger than 2×10^{17} Ne atoms/cm^2. The yield from thick films shows the characteristic sputtering behavior for solid rare gases deposited on a metal substrate,[9,15,16,21] if one extrapolates the yield curve to zero for a bare substrate. The yield below 2×10^{17} Ne atoms/cm^2 may then be composed of contributions from both mechanisms.

A. Yields for thick films

The continuous increase in yield with increasing film thickness above 10^{17} Ne atoms/cm^2 corroborates the idea that a single type of mobile excitation is responsible for the energy transport. (The apparent scattering in individual points reflects different series of measurements rather than actual scattering.) In the following, we shall discuss how the mechanisms in Sec. V C may lead to a yield comparable to the experimental data.

Let us first consider the possibility that the sputtering from solid neon is caused by the formation of mobile molecular excitons and their subsequent diffusion to the surface.[20] We have calculated the energy dependence of

the yield for several values of the diffusion length l_0 on the basis of Eq. (16). The shape of the yield curve is determined by l_0, whereas the absolute magnitude of the calculated yield is adjusted by the value of the product ff_e.

One notes that the curve with $l_0=1\times10^{17}$ Ne atoms/cm^2 (Fig. 6) represents a fair approximation to the experimental data. The positions of the maximum and the shape of the other two curves disagree clearly with the data, however.

The magnitude of l_0 is much less than the length of 1×10^{18} Ne atoms/cm^2 (2500 Å) reported by Pudewill *et al.*,[33] but the discrepancy is acceptable in view of the possible influence of imperfections in our sample. However, the yield evaluated from Eqs. (16) and (17) with $l_0=1\times10^{17}$ Ne atoms/cm^2 and $f=0.35$ and $f_e=1$ becomes about 3.4 Ne atoms/electron for the primary energy $E=2$ keV. This value of f corresponds to mechanism III in Fig. 9 with the ejection of one Ne atom. In this case the yield is approximately a factor of 8 lower than the measured bulk yield. If we use the diffusion length from Pudewill *et al.*,[33] $f=0.35$ and $f_e=1$, the calculated yield for 2 keV is close to the experimental value, but the yield then increases clearly with energy, in complete disagreement with the experimentally determined behavior. In contrast, a calculation with $l_0=1\times10^{17}$ Ne atoms/cm^2 (230 Å) will reproduce the shape of the curve and the position of the maximum fairly well with $ff_e=3$. Thus, our diffusion length is consistent with the overall behavior of the yield, but the suggested mechanism alone cannot explain the magnitude.

The value of $ff_e=3$ is surprisingly large. However, by inserting this value in Eq. (20), one obtains a yield-versus-thickness curve which gradually approaches the curve in Fig. 5. The slope at the origin of the calculated curve is fixed by this choice of ff_e, since all other parameters are known (except l_0, which does not enter the expression in the limit of $d=0$). The agreement between the value of ff_e from the two independent curves, the energy dependence and the thickness dependence of the yield, is very encouraging.

The product ff_e is determined partly by the type of the mobile excitation (f), and partly by the ejection efficiency per deexcitation (f_e). The largest feasible value of f is unity since we have assumed that only one excitation is mobile according to the previous discussion. Then, f_e has to be at least 3.

By the decay of the molecular excitons, we have assumed in Ref. 20 that only one neon atom is ejected, i.e., $f_e=1$. However, the other atom moving into the film may cause sputtering as well. The energy of this atom is sufficient to create a low-energy cascade (cf. Sec. VI C), and the total number of emitted atoms may very well be about the magnitude of the measured yield. In fact, one obtains agreement with the experimental yield if the impact of this atom leads to sputtering of 7–8 atoms from the neon surface. Then $f\approx0.35$ and $f_e\approx8.5$.

Sputtering yields from recent measurements for keV hydrogen-ion bombardment of solid neon demonstrate that the diffusion model is applicable for ion-induced electronic sputtering as well.[61] The energy dependence is fairly well predicted, and as in the case of electrons we obtain satisfactory agreement between the experimental yield and the calculated yield with $ff_e=3$.

Let us now consider the possibility that recombination of molecular holes is the dominant mechanism similar to that reported by Reimann *et al.*[15] for electronic sputtering of solid argon. According to these authors the radiative decay of the molecular excitons to the repulsive ground state (III in Fig. 9) leads to an additional contribution to the sputtering yield.

The holes recombine with prompt or delayed electrons from the substrate. Obviously, the recombination has to take place at or close to the surface in order to provide sufficient energy to the sputtering process. From hole-drift experiments in solid neon it is known that the holes may traverse specimens of more than a few hundreds of micrometers thick.[62] There are apparently no indications in the literature of the characteristic diffusion length of the holes in the absence of any external fields, and of the influence of sample preparation. Le Comber *et al.* point out that the tunneling of a hole Ne_2^+ to a neighboring site is a probable process,[62] which eventually leads to an ordinary diffusion behavior of the holes. However, this particular type of diffusion is not probable in our case. An extrapolation of the hole mobility in neon down to 6 K on the basis of the data and the treatment by Le Comber *et al.*[62] leads to a completely immobile hole.

Nevertheless, let us consider the possibility that recombination might be the dominant process ($f=1$) with a diffusion mechanism different from the one considered by Le Comber *et al.* With $l_0=1\times10^{17}$ atoms/cm^2 as the diffusion length for a hole, we obtain a yield of 10 Ne atoms/electron for incidence of 2-keV electrons from Eqs. (16) and (17). The dependence on energy is, of course, similar to that calculated with $f=0.35$. As in the case of molecular excitons, the dissociative recombination will lead to a yield of about 30 only if one of the atoms causes further sputtering from the neon surface (corresponding to $f_e=3$). The result is based on a complete trapping of the holes at the surface corresponding to the absorbing boundary condition. The use of a highly reflecting boundary as suggested by Reimann *et al.*[15] for the diffusing holes combined with a low-energy cascade model leads to a yield for Ne of about 2 Ne atoms/electron at 2 keV. We shall treat this case in Sec. VI C. We note that although recombination apparently is an important step in the degradation of electronically deposited energy, it does not necessarily mean that dissociative recombination is the dominant source of kinetic energy for sputtering. The energy might as well arise from a combination of transitions from self-trapped molecular and atomic excitons at the surface as the *last step* in the relaxation process initiated by the recombination. We note that the energy supply in both cases is adequate (cf. Sec. V C), but that the use of Eq. (16) without modification means that the excitons have to remain close to the surface where the recombination took place.

The importance of recombination is illustrated by Fig. 2. The effect of a positive bias is primarily that all internal low-energy secondary electrons disappear from the neon film because of the negative affinity of solid neon,

before they may recombine. This means that the sample may charge up positively relative to the metal substrate. When the potential of the film is sufficiently high, the internal secondaries do not leave the film or electrons from the substrate are attracted by the positive region in the film. The sputtering begins when the electrons start to recombine. This explanation would be consistent with the apparent delay in erosion with a positive bias.

We do not consider the contribution from deexciting atomic excitons to be substantial. The reason is primarily the low-energy release from this transition estimated by the considerations in Sec. V C.

For solid neon recent measurements[63] indicate that the sputtering by eV electrons starts close to the threshold for exciton production (≈ 17 eV), whereas no strong enhancement is observed for energies close to the band gap. This observation supports the suggestion that decaying excitons are the dominant energy source for the particle ejection.

Although so far we have considered one dominant mobile excitation, one cannot exclude that two types of mobile excitations with different diffusion length contribute to the sputtering. For example, hole diffusion prior to recombination may broaden the initial Gaussian distribution of excitations. The resulting distribution of mobile excitons leads to a second diffusion of excitations, which may behave similarly to the assumptions in Sec. V. Then, the necessary energy for the sputtering is essentially provided by decaying, surface-trapped molecular, or atomic $3s$ excitons, i.e., via mechanism IV + III in Fig. 9 or by strain minimization as suggested by Coletti *et al.*[12]

B. Yields for thin films

The strong enhancement of the yield for thicknesses below 5×10^{16} Ne atoms/cm^2 has not been observed for other condensed gases at present. Recent measurements indicate that this thin-film behavior is found for incidence of keV hydrogen ions as well.[61] Thus, we are led to the conclusion that the strong enhancement for small thicknesses is primarily a property of the neon film on a metal substrate, but is not influenced much by the type of the primary particle or the spectrum of backscattered particles. In this connection, we note that the contribution from backscattered electrons for irradiation of solid oxygen was significant up to one-half of the electron range.[17] For neon, the contribution from these electrons are hidden in the complex depth dependence.

The possibility exists that the high yield for these small thicknesses is caused by a violent process with a small effective range from the substrate. A yield of about 100 Ne atoms/electron has even been observed for these thin films. In view of the sublimation energy of 20 meV, it means that the resulting process has to liberate at least approximately 2 eV, unless emission of clusters takes place.

Cluster formation for thin neon films might be another reason for the high yield. The films are more or less uniform for thicknesses above 5×10^{16} Ne atoms/cm^2, whereas films below this thickness show a strong tendency to form clusters.[64] We may not exclude that kinetic energy, e.g., released from a dissociative recombination, is consumed very effectively for erosion of clusters.

C. Comparisons with models for a reflecting surface

Let us compare the present results with two models in which the surface acts as a reflecting boundary, sputtering from low-energy cascades or spherical spikes. The energy-releasing processes may be dissociative recombination or decay of molecular excitons as described above.

Ordinary sputtering theory was extended to electronic sputtering for electron irradiation of solid oxygen and nitrogen by Ellegaard *et al.*[17] It turned out that this *low-energy cascade* model explained the energy dependence of the yield as well as its approximate magnitude for primary electrons. The yield is essentially determined by the surface value $D_e(0)$ of the distribution $D_e(x)$ of energy deposited in electronic excitations. The derivation in Refs. 17 and 49 gave the important result that the yield caused by particle bombardment for medium and low excitation densities is

$$\tfrac{1}{2}[D_e(0)/W]E_s\Lambda \text{ (atoms/primary)} . \tag{23}$$

E_s is the energy release for example by an electronic deexcitation. The constant Λ is determined by properties of the target material alone, e.g., the sublimation energy U_0 and the low-energy stopping power for atoms.[13] A similar expression involving a treatment based on low-energy cascades has been presented by Johnson and Brown,[65] and Garrison and Johnson.[66] Equation (23) is determined by the distribution of isotropic sources of released energy for these low-energy cascades. The surface density for nonmobile sources is $D_e(0)/W$, e.g., as in solid nitrogen, but for solid neon the source distribution is different from the distribution of electronically deposited energy due to the mobility of the excitations. However, if the excitations are reflected at the surface, one may estimate the simple case of a primary with constant stopping power. The two distributions are identical apart from a constant factor up to quite large depths, provided that the diffusion length is much smaller than the range of the particle. One may evaluate the yield from Eq. (23) for 1.5-MeV protons incident on solid argon to $Y=1.5$ Ar atoms/H$^+$ compared to the experimental yield $Y=2.2$ Ar atoms/H$^+$.[15,16] Here we applied $D_e(x)=NS_e(E)$ and an energy release $E_s=2$ eV, which is a typical value for argon.[15]

Let us shortly estimate the yield for 2-keV electrons incident on solid neon on the basis of this low-energy cascade model. The spatial distribution of deexciting states is broadened from the original Gaussian distribution $G(x)$, Eq. (15b), corresponding to a diffusion with the characteristic length $l_0=1\times10^{17}$ Ne atoms/cm^2. We approximate this distribution of internal sources by a constant excitation density of $2NS_e(E)$. Then, we obtain, for example, for mechanisms III ($f=0.35$) in Fig. 9, $\Lambda=49$ Å/eV and the yield $Y=1.6$ Ne atoms/electron. This yield is almost 1 order of magnitude too small, although we have used relatively high values as input parameters, e.g., an energy release of $E_s=3.7$ eV and an excitation density of $2NS_e$. As usual, the energy W required to produce an ion-electron pair has been set equal to 35 eV,[18,20] and for Λ the usual power approximation[13] has been used.

Rather than treating the deexciting particles as a center for a low-energy cascade we may consider the possibility

for *low-energy spherical spikes*[18,67] around such a center. The contribution from these elastic collision spikes may be appreciable for large values of the energy release E_s compared with the sublimation energy U_0. However, the yield from this model does not exceed 3.5 Ne atoms/electron even for the high input parameters used in the previous case for low-energy cascades.

The yield evaluation may lead only to values close to the experimental yield, if the cross section in Λ and in the corresponding evaluation of the spherical collision spike is replaced by a cross section 1 order of magnitude lower than its given value. Although the interaction between low-energy neon nuclei is comparatively weak, one may hardly expect such a pronounced deviation from the standard cross section.

D. Influence of impurities

The apparent delay of the erosion for the doped films (Fig. 6) is probably caused by a less efficient diffusion of the mobile excitation. The measurement of the pure film leads, as usual, to a yield of about 30 Ne atoms/electron, whereas the contaminated films apparently have a small erosion rate during the initial stage of the irradiation. However, one should note that we do not observe a clear correlation between increasing impurity concentration and decreasing sputtering yield, as Brown *et al.* did for oxygen impurities in solid argon.[16]

VII. CONCLUSION

Films of solid neon with thicknesses of 2×10^{16} up to 2×10^{18} Ne atoms/cm^2 have been irradiated by primary electrons at energies from 0.8 to 3 keV. Measurements of erosion yields, particularly of the yield for electronic sputtering, have been carried out by the frequency-change method and the emissivity-change method. The agreement between these two methods was fairly good. The yield for 2-keV electrons incident on thick films is about 30 Ne atoms/electron. The yield decreases with decreasing film thickness to about 10 Ne atoms/electron at the thickness 5×10^{16} Ne atoms/cm^2. This indicates the existence of a long-range diffusion of excitations which provide atoms close to the surface with the necessary energy for the sputtering process. The characteristic diffusion length is approximately 1×10^{17} Ne atoms/cm^2 ($\approx$230 Å). For very thin films a strong enhancement of the yield was observed.

The energy dependence of the bulk yield is consistent with the suggested diffusion length. There is a maximum in the yield at energies for which the primary electrons have a range comparable to the diffusion length. Above 1.5 keV the bulk yield is proportional to the stopping power for the primary electrons.

All measurements of the electronic sputtering yield have been performed at temperatures below about 6 K. A significant evaporation occurs for elevated temperatures. These latter measurements were performed on a massive gold substrate in order to obtain a satisfactory temperature determination. Doping of neon films with argon leads to a clear delay in the erosion.

The model presented previously for diffusion and decay of excitons has been extended to a general transport model of excitations to the surface with subsequent trapping and energy release for sputtering. The treatment for constant excitation density has been modified to include the distribution of electronically deposited energy for primary keV electrons. The electronic deexcitation is probably initiated by dissociative recombination, which may or may not be the dominant energy-releasing process. On the other hand, the important process might just as well be the radiative decay of self-trapped atomic or molecular excitons to a repulsive ground state. However, the suggested decay may hardly be responsible alone for such a large bulk yield without contributions from low-energy cascades initiated at the surface. This subsequent sputtering by surface-trapped deexciting particles with yields from about 10 to 3 Ne atoms/neon-atom may account for the observed yield of 20—40 Ne atoms/electron in our energy regime. The model is based on an absorbing surface as a boundary condition. The use of a highly reflecting surface as a boundary condition does not lead to satisfactory agreement with the experimental results in contrast to the case of MeV protons incident on solid argon.

Direct sputtering from electron-nucleus collisions in solid neon does not contribute significantly to the thick-film yield because of the very low cross section. Beam-induced evaporation may be neglected for current densities below 10 μA/cm^2.

ACKNOWLEDGMENTS

The authors have appreciated discussions with P. Sigmund, G. Zimmerer, W. L. Brown, R. Pedrys, R. E. Johnson, J. M. Debever, and F. Coletti. We thank as well J. M. Debever and F. Coletti for giving us the opportunity to include their unpublished work in our discussion. We acknowledge the technical staff, A. Nordskov and B. Sass, for competent assistance. We have appreciated the help of K. Weisberg in designing the electronic equipment. The work of one of us (C.C.) has been made possible by a research grant from the Danish Natural Science Research Council.

*Present address: Max-Planck-Institut für Plasmaphysik, D-8046 Garching bei München, Federal Republic of Germany.

[1]T. A. Tombrello, Radiat. Eff. **65**, 149 (1982).

[2]R. E. Johnson, L. J. Lanzerotti, W. L. Brown, W. M. Augustyniak, and C. Mussil, Astr. Astrophys. **123**, 343 (1983).

[3]R. A. Haring, A. W. Kolfschoten, and A. E. de Vries, Nucl. Instrum. Methods B **2**, 544 (1984).

[4]O. Gröbner and R. S. Calder, IEEE Trans. Nucl. Sci. **NS-20**, 760 (1973).

[5]S. L. Milora, J. Fus. Energy **1**, 15 (1981).

[6]C. T. Chang, L. W. Jørgensen, P. Nielsen, and L. L. Lengyel,

Nucl. Fus. **20**, 859 (1980).
[7]J. Schou, H. Sørensen, and P. Børgesen, Nucl. Instrum. Methods B **5**, 44 (1984).
[8]T. A. Tombrello, in *Desorption Induced by Electronic Transitions,* edited by N. H. Tolk, M. M. Traum, J. C. Tully, and T. E. Madey (Springer, Berlin, 1983), p. 239.
[9]F. Besenbacher, J. Bøttiger, O. Graversen, J. L. Hansen, and H. Sørensen, Nucl. Instrum. Methods **191**, 221 (1981).
[10]W. L. Brown, W. M. Augustyniak, K. J. Marcantonio, E. H. Simmons, J. W. Boring, R. E. Johnson, and C. T. Reimann, Nucl. Instrum. Methods B **1**, 307 (1984).
[11]R. Pedrys, R. A. Haring, A. Haring, F. W. Saris, and A. E. de Vries, Phys. Lett. **82A**, 371 (1981).
[12]F. Coletti, J. M. Debever, and G. Zimmerer, J. Phys. (Paris) Lett. **45**, L467 (1984).
[13]P. Sigmund, in *Sputtering by Particle Bombardment I,* edited by R. Behrisch (Springer, Berlin, 1981), p. 9.
[14]R. E. Johnson and M. Inokuti, Nucl. Instrum. Methods **206**, 289 (1983).
[15]C. T. Reimann, R. E. Johnson, and W. L. Brown, Phys. Rev. Lett. **53**, 600 (1984).
[16]W. L. Brown, C. T. Reimann, and R. E. Johnson, in *Desorption Induced by Electronic Transitions, DIET II,* edited by W. Brenig and D. Menzel (Springer, Berlin, 1985), p. 199.
[17]O. Ellegaard, J. Schou, H. Sørensen, and P. Børgesen, Surf. Sci. **167**, 474 (1986).
[18]C. Claussen, Ph.D. thesis, University of Odense, 1982 (unpublished).
[19]M. Szymonski, J. Ruthowski, A. Poradzisz, Z. Postawa, and B. Jørgensen, in *Desorption Induced by Electronic Transitions, DIET II,* Ref. 16, p. 160.
[20]P. Børgesen, J. Schou, H. Sørensen, and C. Claussen, Appl. Phys. A **29**, 57 (1982).
[21]R. W. Ollerhead, J. Bøttiger, J. A. Davies, J. l'Ecuyer, H. K. Haugen, and N. Matsunami, Radiat. Eff. **49**, 203 (1980).
[22]R. Pedrys, D. J. Oostra, and A. E. de Vries, in *Desorption Induced by Electronic Transitions, DIET II,* Ref. 16, p. 190.
[23]F. Coletti and J. M. Debever, Solid State Commun. **47**, 47 (1983).
[24]R. E. Packard, F. Reif, and C. M. Surko, Phys. Rev. Lett. **25**, 1435 (1970).
[25]F. Coletti and A. M. Bonnot, Chem. Phys. Lett. **55**, 92 (1978).
[26]I. Ya. Fugol', Adv. Phys. **27**, 1 (1978).
[27]F. Coletti, J. M. Debever, and G. Zimmerer, J. Chem. Phys. **83**, 49 (1985).
[28]N. Schwentner, E.-E. Koch, and J. Jortner, *Electronic Excitations in Condensed Rare Gases* (Springer, Berlin, 1985).
[29]V. Saile and E.-E. Koch, Phys. Rev. B **20**, 784 (1979).
[30]R. Gaethke, P. Gürtler, R. Kink, E. Roick, and G. Zimmerer, Phys. Status Solidi B **124**, 335 (1984).
[31]E. Schuberth and M. Creuzburg, Phys. Status Solidi B **71**, 797 (1975).
[32]E. Roick, R. Gaethke, P. Gürtler, T. O. Woodruff, and G. Zimmerer, J. Phys. C **17**, 945 (1984).
[33]D. Pudewill, F.-J. Himpsel, V. Saile, N. Schwentner, M. Skibowski, E.-E. Koch, and J. Jortner, J. Chem. Phys. **65**, 5226 (1976).
[34]H. Sørensen and J. Schou, J. Appl. Phys. **49**, 5311 (1978).
[35]M. Øhlenschlaeger, H. H. Andersen, J. Schou, and H. Sørensen, Radiat. Prot. Dosim (to be published).
[36]P. Børgesen, J. Schou, H. Sørensen, and O. Ellegaard (unpublished).
[37]D. Cherns, Surf. Sci. **90**, 339 (1979).
[38]M. J. Berger, S. M. Seltzer, and K. Maeda, J. Atm. Terr. Phys. **32**, 1015 (1970).
[39]W. L. Brown, W. M. Augustyniak, L. J. Lanzerotti, R. E. Johnson, and R. Evatt, Phys. Rev. Lett. **45**, 1632 (1980).
[40]J. W. Boring, R. E. Johnson, C. T. Reimann, J. W. Garrett, W. L. Brown, and K. J. Marcantonio, Nucl. Instrum. Methods **218**, 707 (1983).
[41]J. W. Boring, J. W. Garrett, T. A. Cummings, R. E. Johnson, and W. L. Brown, Nucl. Instrum. Methods B **1**, 321 (1984).
[42]S. K. Erents and G. M. McCracken, J. Appl. Phys. **44**, 3139 (1973).
[43]P. Sigmund and M. Szymonski, Appl. Phys. A **33**, 141 (1984).
[44]M. Urbassek and P. Sigmund, Appl. Phys. A **35**, 19 (1984).
[45]T. Nakayama, M. Okigawa, and N. Itoh, Nucl. Instrum. Methods B **1**, 301 (1984).
[46]Z. Ophir, B. Raz, J. Jortner, V. Saile, N. Schwentner, E.-E. Koch, M. Skibowski, and W. Steinmann, J. Chem. Phys. **62**, 650 (1975).
[47]N. Schwentner, G. Martens, and H. W. Rudolf, Phys. Status Solidi B **106**, 183 (1981).
[48]J. Schou, Phys. Rev. B **22**, 2141 (1980).
[49]O. Ellegaard, Ph.D. thesis, Risø National Laboratory, 1986 (unpublished).
[50]H. Niedrig, Scanning **1**, 17 (1978).
[51]S. Valkealahti and R. Nieminen (private communication).
[52]A. E. S. Green and L. R. Peterson, J. Geoph. Res. **73**, 233 (1968).
[53]A. G. Belov, E. M. Yurtaeva, and V. N. Svishchev, Fiz. Nizk. Temp. **7**, 350 (1981) [Sov. J. Low Temp. Phys. **7**, 172 (1981)].
[54]K. Inoue, H. Sakamoto, and H. Kanzaki, Solid State Commun. **44**, 1007 (1982).
[55]K. Inoue, H. Sakamoto, and H. Kanzaki, Solid State Commun. **49**, 191 (1984).
[56]T. Doke, A. Hitachi, S. Kobota, A. Nakamoto, and T. Takahashi, Nucl. Instrum. Methods **134**, 353 (1976).
[57]L. R. Peterson and A. E. S. Green, J. Phys. B **1**, 1131 (1968).
[58]L. Frommhold and M. A. Biondi, Phys. Rev. **185**, 244 (1969).
[59]I. Ya. Fugol' and E. I. Tarasova, Fiz. Nizk. Temp. **3**, 366 (1977) [Sov. J. Low Temp. Phys. **3**, 176 (1977)].
[60]M. Selg, Phys. Status Solidi B **129**, 775 (1985).
[61]O. Ellegaard, J. Schou, and H. Sørensen, Nucl. Instrum. Methods B **13**, 567 (1986).
[62]P. G. Le Comber, R. J. Loveland, and W. E. Spear, Phys. Rev. B **11**, 3124 (1975).
[63]J. M. Debever and F. Coletti (private communication).
[64]J. Krim (private communication); J. Krim, J. G. Dash, and J. Suzanne, Phys. Rev. Lett. **52**, 640 (1984).
[65]R. E. Johnson and W. Brown, Nucl. Instrum. Methods **198**, 103 (1982).
[66]B. J. Garrison and R. E. Johnson, Surf. Sci. **148**, 388 (1984).
[67]C. Claussen, Nucl. Instrum. Methods **194**, 567 (1982).